ISSN 0965-545X, Polymer Science, Series A, 2018, Vol. 60, No. 3, pp. 342–349. © Pleiades Publishing, Ltd., 2018.

POLYMER BLENDS

Effect of Supercritical Carbon Dioxide Conditions on PVDF/PVP Microcellular Foams[1]

Yanhui Xiang[a,*] and Haibo Lin[b]

[a] *Jiaxing Nanyang Polytechnic Institute, Jiaxing, 314031 China*

[b] *Ningbo Institute of Materials Technology and Engineering, Chinese Academy of Sciences, Ningbo, 315201 China*

**e-mail: xiangyh1989@163.com*

Received July 15, 2017;
Revised Manuscript Received December 18, 2017

Abstract—Supercritical carbon dioxide ($ScCO_2$) was used as a physical foaming agent to prepare poly(vinylidene fluoride)/poly(*N*-vinyl pyrrolidone) (PVDF/PVP) microstructure material. The effects of foaming conditions including saturation pressure, foaming temperature and foaming time on PVDF/PVP foams morphology, thermal and electrical behavior were systematically investigated by scanning electron microscope, differential scanning calorimeter and broadband dielectric spectrometer. Small cell and low cell density were achieved at low pressure of 12 MPa, as increasing saturation pressure, the average cell size increased first, and then decreased. The competition between the cell growth and cell nucleation played an important role in average cell size, which was directly related to $ScCO_2$ processing conditions. With increasing foaming temperature, cell size was increased and cell density was decreased, in a nearly linear manner. The variation of foaming time was considered to be closely related to the time for cells to grow. Thus, the results revealed that the average cell size enhanced with extending foaming time. The thermal properties of PVDF/PVP composites are slightly influenced by foaming parameters, and the dielectric constant of PVDF/PVP composite foams decreased with increasing volume expansion ratio.

DOI: 10.1134/S0965545X18030161

INTRODUCTION

Due to the advantages such as lightweight, buoyancy, cushioning performance, thermal and acoustic insulation, impact damping, and cost reduction [1], polymeric foams can be widely used in manifold fields like packaging, acoustic absorbents, automotive parts, as well as sporting equipment and construction industries [2, 3]. However, a major drawback of polymeric foams compared to their bulk counterparts is the sacrifice of inferior mechanical strength and thermal stability, which limit their further advanced applications. In order to overcome these shortcomings, the average cell size needs to be decreased and the cell density needs to be high enough. For this reason, the microcellular foams which have the average cell size less than 10 um and cell density higher than 10^9 cells/cm^3 are developed and attract much attention, this type of foams possess a relatively low density ranging from 0.05–0.95 g/cm^3 and do not sacrifice the mechanical strength [4, 5]. Moreover, they can offer the materials with a much higher impact strength and anti-fatigue property compared to the bulk counterparts.

Nevertheless, producing polymeric foams with small cell size and high cell density is not easy. Generally, high concentrated blowing agent in polymer is essential, which always results in high pressure and large pressure drop rate. Another method for modifying cell morphology and density is to add nucleation agents, which benefit the formation of embryo, and hence produce high cell density and small cell size.

Supercritical carbon dioxide ($ScCO_2$) is an environmentally friendly, chemical inert, inexpensive and versatile solvent and a promising alternative to noxious organic solvents [6–9]. In the past few decades, it has attracted particular attention as a supercritical fluid in chemical synthesis and in processing areas for polymers due to its appealing and unique properties. A variety of works has been done on the swelling of polymer/CO_2 solution [10–12], the solubility and diffusivity [13–16] of CO_2 in polymers. Furthermore, the incorporation of CO_2 into polymer seemed to be an efficient route to reduce greenhouse gas pollution and

[1] The article is published in the original.

overcome the shortages in petroleum. More and more researches have focused on $ScCO_2$ as a physical foaming agent to generate microcellular material with high cell density and low average cell size.

Many studies have been done on polymer composite foams [17–21]. Microcellular foaming technology involved CO_2 was applied by Zheng's group to fabricate poly(lactic acid) (PLA)/silica nanocomposite foams with high crystallinity, uniform cell morphology, and high expansion ratio [22]. The introduction of nanosilica was verified to significantly improve the foaming behavior of PLA. The influence of nanosilica on foams morphology was also studied by Rahmi Ozisik and co-workers. It was found out that nanosilica worked as nucleating agents. The application of nanosilica provides an interface, upon which CO_2 nucleates and leads to remarkably low average cell sizes while improving cell density [23]. The fabrication of well-controlled porous foams of graphene oxide modified poly (propylene-carbonate) using supercritical carbon dioxide was studied by Fu's group [24]. The results indicated that incorporation of graphene oxide increased the polymer's glass transaction temperature by 10°C and the storage modulus by 50 times. It was demonstrated that the nanocomposite foams had good dimension stability and the final pore features were depended on $ScCO_2$ saturation conditions. In addition, cytotoxicity and in vitro cell culturing tests of selected foams showed that the fabricated porous materials were non-cytotoxic and able to support cellular adhesion within 3D structure, suggesting that these were promising materials for tissue engineering applications.

Semi-crystalline poly(vinylidene fluoride) (PVDF) has been widely applied to produce ultrafiltration and microfiltration membranes with regard to its outstanding properties such as high mechanical strength, thermal stability, chemical resistance and high hydrophobicity [25–31]. The application of this material as foams is still rare. It remains to be challenging to fabricate semi-crystalline polymeric foam with a high expansion ratio and well-defined cell structure. Herein, we produced PVDF/poly(*N*-vinyl pyrrolidone) PVP composite foams using $ScCO_2$ as physical foaming agent. The function of PVP is to increase the amount of amorphous phase. Such, the solubility of $ScCO_2$ in polymer system enhanced, which leading to high cell density and uniform cell. The effects of foaming condition including saturation pressure, foaming temperature and foaming time on PVDF/PVP foams morphology, thermal and electrical behavior were investigated by SEM, DSC and electrochemical potentiostat in details.

EXPERIMENTAL

Materials

PVDF (FR904) was supplied by Shanghai 3F New Material Co., Ltd. China. PVP (K90) was supplied by Shanghai Aladdin Chemistry Co., Ltd. China. They were dried at 80°C in a vacuum oven for 24 h before use. CO_2 was obtained from Ningbo Wanli Gas Corporation with a purity of 99.9% and used as physical foaming agent.

Sample Preparation

95 wt % PVDF and 5 wt % PVP composites were compounded using a Brabender mixer at 200°C under 50 rpm. Specimens with a thickness of 1 mm were prepared by compression molding at 200°C, 15 MPa and quenched to room temperature by cold water. Then the sheets were cut into specimens with dimensions of 25 × 25 mm for further foaming experiments.

Preparation of PVDF/PVP Composite foams by $ScCO_2$

The prepared PVDF/PVP specimens (25 × 25 mm) were transferred into a high pressure vessel (internal volume ~40 cm^3), which was preheated to settled temperature. After the sealing process was accomplished, the vessel was flushed with CO_2 for 3 min to eliminate the original air and then pressurized with CO_2 to the required pressure using a high-pressure pump. The samples were treated under these conditions for varied time. Finally, the vessel was depressed rapidly within 30 s and PVDF/PVP composite foams were obtained. Preparation conditions with varied processing pressure, temperature and foaming time are summarized in Table 1.

Characterization of PVDF/PVP Composite Foams

Morphological structures as well as cell size distribution of the prepared PVDF/PVP foams were determined by a Hitachi TM-1000 scanning electron microscope (SEM). The mass densities of the samples before ρ and after ρ_f foaming were measured by the water displacement method based on ISO 1183-1987. The uptake of water by the samples during this measurement can be neglected due to the samples' smooth skin and closed cells. The volume expansion ratio V_f of the polymer foam can be calculated according to Eq. (1) as follows:

$$V_f = \frac{\rho - \rho_f}{\rho}, \quad (1)$$

where ρ and ρ_f are the mass densities of the samples before and after foaming respectively.

Table 1. Foaming conditions of PVDF/PVP composite foams

Sample name	Temperature, °C	Pressure, MPa	Foaming time, min
SP-P12	230	12	10
SP-P16	230	16	10
SP-P20	230	20	10
SP-P24	230	24	10
SP-P28	230	28	10
SP-P32	230	32	10
SP-T200	200	28	15
SP-T210	210	28	15
SP-T220	220	28	15
SP-T230	230	28	15
SP-t15	210	27	15
SP-t30	210	27	30
SP-t45	210	27	45

Cell size and cell density (the number of cells per cubic centimeter of solid polymer) were determined from SEM images using software Image-Pro Plus, and at least 100 cells were counted on the SEM images to calculate a mean value. The cell density ρ_c was determined according to Eq. (2) as follows:

$$\rho_c = \left[\frac{nM^2}{A}\right]^{3/2}\left[\frac{1}{1-V_f}\right], \quad (2)$$

where n is the number of cells in the micrograph, M is the magnification factor, A is the area of the micrograph (cm^2), and V_f is the expansion ratio of the foam.

The melt temperature and crystallinity of the composite foams were determined by differential scanning calorimeter (DSC, Pyris Diamond, Perkin Elmer, US) equipped with a cooling apparatus under a nitrogen atmosphere at a heating rate of 10 °C/min over the range of 30–250°C. Crystallinity of the composite foams was calculated by dividing the measured heat of fusion ΔH_f by the value of perfect PVDF crystal ($\Delta H_0 = 105$ J/g) reported in the literature [32].

The dielectric constant ε was measured using a broadband dielectric spectrometer system Concept 80 (Novocontrol). The PVDF/PVP microcellular foam was cut into specimens with area of 1 cm^2, and the thickness was unchanged just after foam process, both sides of the sample were coated by gold. The measurement temperature was set at 25°C, and the voltage maintained at 500 mV. The frequency range was from 10 to 10^7 Hz.

RESULTS AND DISCUSSION

The Effect of Foaming Pressure on PVDF/PVP Composites

The effect of pressure on morphologies of PVDF/PVP composite foams was investigated by SEM, while keeping the foaming temperature at 230°C and foaming time of 10 min. As shown in Fig. 1a, the average cell size and cell density varied significantly with increasing the pressure from 12 to 32 MPa. Pressure variation is closely related to the solubility power of CO_2 in PVDF/PVP composites [24]. With increasing pressure from 12 to 20 MPa, the average cell size increased from 43.21 to 57.74 μm due to the enhanced solubility of $ScCO_2$ in PVDF/PVP composite and decreased system viscosity, as shown in Fig. 1b. Nevertheless, when further increasing pressure form 20 to 32 MPa, the average cell size decreased from 57.74 to 18.78 μm, and the cell density increased from 1.18×10^8 to 32.10×10^8. Under higher saturation pressure, CO_2 solubility in PVDF/PVP is getting higher to reduce the free energy barriers for nucleation, which subsequently leads to the formation of more nucleations. Besides, the higher pressure drop rate limits the further growth of nucleations, therefore, decreasing cell size and increasing cell density are observed as illustrated in Fig. 1a (from SP-P20 to SP-P32) and Fig. 1b. The foams' volume expansion ratio varies with the pressure in a similar trend with average pore size, while the cell bulk density varies in an opposite way, as shown in Fig. 1c. The cell size distribution is also demonstrated in Fig. 2, and it could be seen that

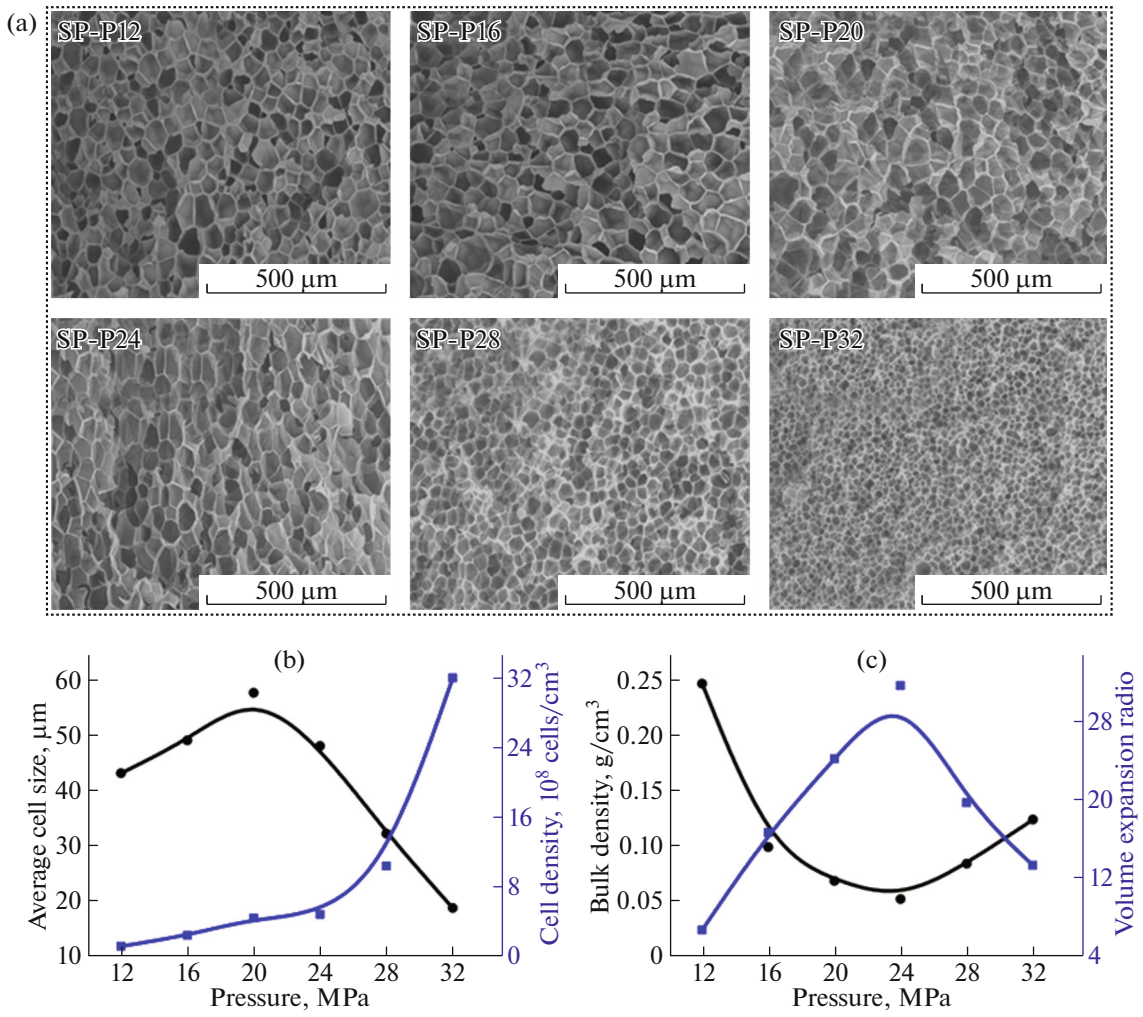

Fig. 1. (Color online) (a) SEM images of PVDF/PVP foams produced at different pressure; (b) average cell size and cell density of PVDF/PVP composite foams produced at different pressure; (c) the bulk density and volume expansion ratio of PVDF/PVP foams produced at different pressure.

the distribution of SP-32 is getting narrower and more uniform with increasing the pressure, which is in good accordance with SEM picture in Fig. 1a.

Thermal behavior of PVDF/PVP foams was studied by DSC; results are summarized in Table 2. It was found that T_m (around 160°C) and T_c (around 119°C) are almost not influenced by foaming pressure. On the basis of the area of the heating curves measured by DSC, the degree of crystallinity X_c values of PVDF/PVP foams were calculated, and the crystallinity of SP-P20 with largest average cell size reaches 41.7%, which is mainly dominated by the cell growth surpassing nucleation.

The Effect of Foaming Temperature on PVDF/PVP Composites

The influence of the foaming temperature on foam morphology was studied as the temperature increased from 200 to 230°C at a constant saturation pressure of 28 MPa and foaming time of 15 min, respectively. SEM images of PVDF/PVP composite foams prepared at different temperature are depicted in Fig. 3a, and all foams exhibit a circular-pore structure. It is obvious that, the average cell size is enhanced with increasing foaming temperature. Detailed variations of cell structure features such as the average cell size, cell density, bulk density and volume expansion ratio with the foaming temperature for PVDF/PVP can be seen in Figs. 3b, 3c. It is evident that with increasing temperature, PVDF/PVP foams showed an apparent increase in cell size, which is 12.64 μm at 200°C and 22.21 μm at 230°C, nearly two times larger. This change in cell size is related with the system viscosity and sight decreased content of $ScCO_2$ in PVDF/PVP composites. It is well known that, as temperature increased, the viscosity of the polymer matrix decreased to facilitate the foaming. In addition,

greater diffusion of $ScCO_2$ under higher temperature could facilitate the growth and expansion of pores. Furthermore, at high temperature, the solubility of $ScCO_2$ in system decreased as well as melting strength. In this case, the growth and combination of cell play a dominant role, thus increased cell size and decreased cell density are observed. Due to the increased cell size and decreased cell density at high temperature (230°C), the bulk density dropped from 0.304 to 0.145 g/cm^3.Opposite trend was observed for volume expansion ratio of the foams, which promoted from 5.44 to 11.33 as foaming temperature increased from 200 to 230°C. The average cell size distribution is also performed in Fig. 4; the wider distribution implied a decreased uniformity of cell structure at high temperature.

Thermal behavior of PVDF/PVP foams produced at different temperature was also explored by DSC and the result are shown in Table 2. The melting temperature of SP-T210 is 165.7°C, a little higher than for other samples. The crystallization temperature of the samples prepared at varied temperature is around 128°C. All these results indicate that the as-prepared PVDF/PVP foams have stable thermal properties at varied foaming temperature.

The Effect of Foaming Time on PVDF/PVP Composites

Another adjustable parameter influencing foam morphology is foaming time. It was studied by comparing foams prepared with a foaming time of 15, 30, and 45 min at a foaming temperature of 210°C and a saturation pressure of 27 MPa. SEM results given in Fig. 5a indicate that with increasing foaming time from 15 to 45 min, the average cell size enlarged. Figure 5b quantitatively shows the average cell size which increases from 16.08 to 28.96 μm. It is believed that longer foaming time results in more sorption of CO_2. As previously mentioned the increased adsorption quantity of CO_2 decreases the viscosity of composites and increases the period of pore growth. In this case, the cell density decreases from 2.53×10^9 to 0.97×10^9 cells/cm^3.It is widely accepted that both the cell density and cell size affect the bulk density. Here the bulk density decreased from 0.218 to 0.143 g/cm^3 as extended foaming time from 15 to 45 min. This behavior of bulk density is mainly due to the competition between cell nucleation and cell growth. In this case, cell growth played a dominant role in the determination of the bulk density. The expansion ratio is also a critical data to present the foaming behavior of polymers, and a high expansion ratio can effectively reduce the resin dosage. From the results in Fig. 5c, the volume expansion ratio changed from 7.6 with foaming time of 15 min to 11.6 with foaming time of 45 min, implying a significant effect of foaming time on polymer foaming behavior. The variation of average cell size distribution shown in Fig. 6a is not obvious, implying a relative uniform morphology during foaming process.

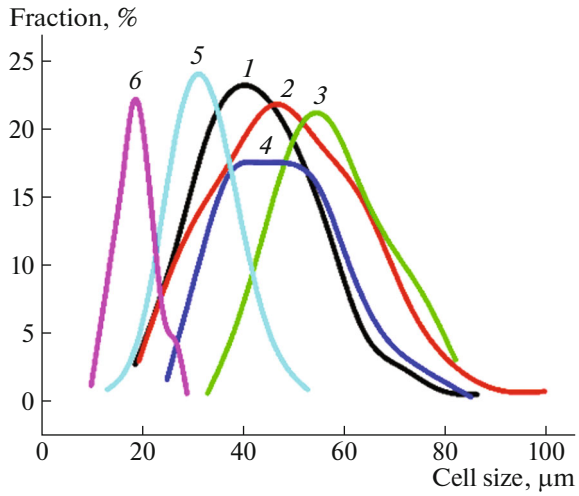

Fig. 2. (Color online) The cell size distribution of PVDF/PVP composite foams produced at different pressure: (*1*) SP-P12, (*2*) SP-P16, (*3*) SP-P20, (*4*) SP-P24, (*5*) SP-P28, (*6*) SP-P32.

The thermodynamic parameters resulting from the DSC study are summarized in Table 2. The melting temperature of SP-t15 and SP-t30 is very close, however when foaming time extended to 45 min, T_m decreased to 161.5°C. During DSC cooling down pro-

Table 2. Thermal behavior of PVDF/PVP foams produced at different conditions

Sample name	T_m, °C	T_c, °C	Crystallinity, %
SP-P12	159.3	119.4	35.9
SP-P16	161.3	119.0	32.7
SP-P20	157.8	119.4	41.7
SP-P24	163.1	118.8	34.6
SP-P28	159.6	119.2	39.3
SP-P32	160.1	118.9	37.4
SP-T200	161.3	127.5	39.9
SP-T210	165.7	128.3	42.4
SP-T220	161.4	128.8	43.8
SP-T230	162.7	128.0	36.6
SP-t15	165.5	129.2	40.9
SP-t30	166.7	130.7	43.7
SP-t45	161.5	128.2	43.7

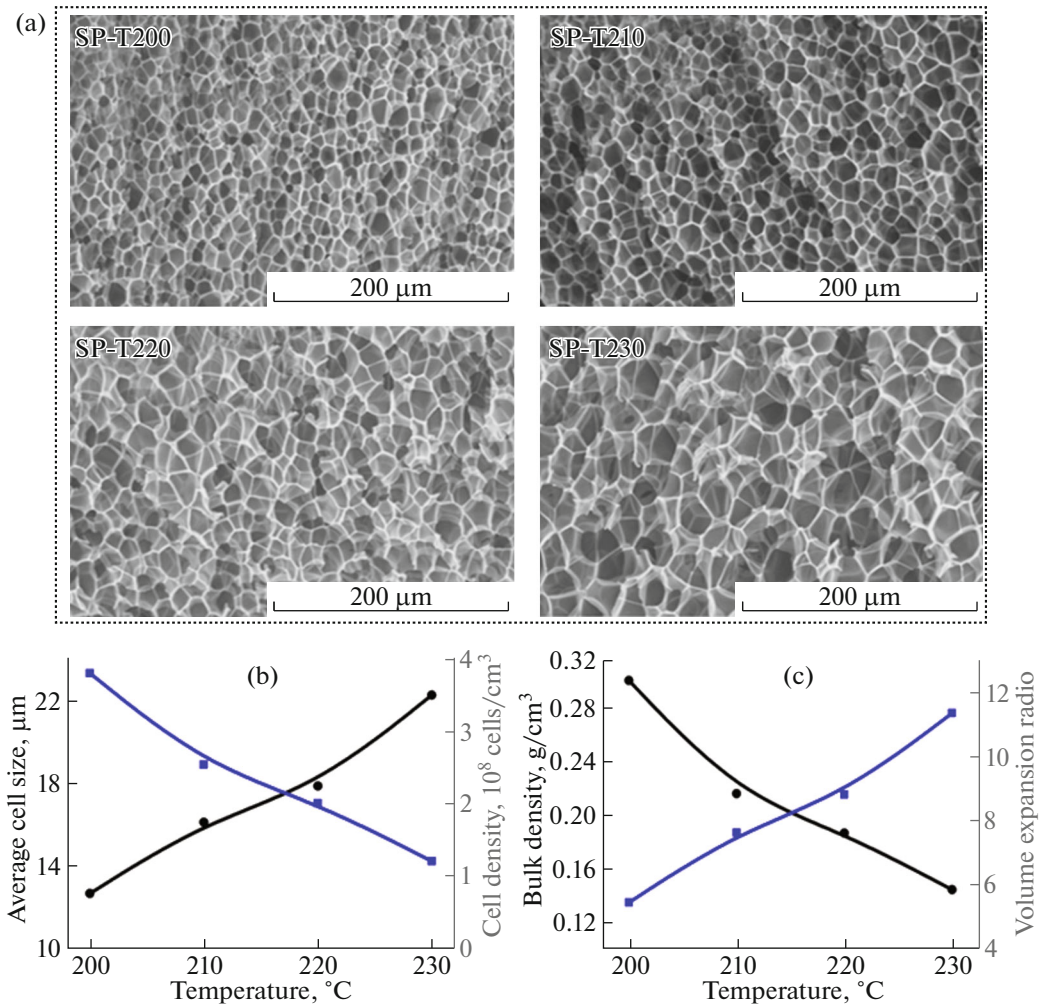

Fig. 3. (Color online) (a) SEM images of PVDF/PVP foams produced at different temperature; (b) average cell size and cell density of PVDF/PVP foams produced at different temperature; (c) the bulk density and volume expansion ratio of PVDF/PVP foams produced at different temperature.

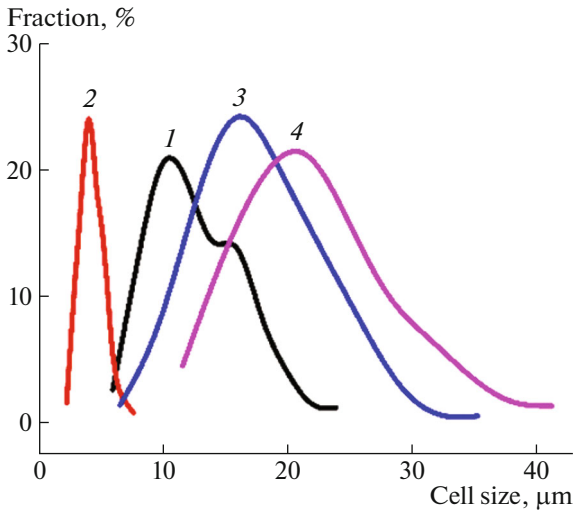

Fig. 4. (Color online) The cell size distribution of PVDF/PVP foams produced at different temperature: (*1*) SP-T200, (*2*) SP-T210, (*3*) SP-T220, (*4*) SP-T230.

cess, T_c and crystallinity were measured, and the value showed slight relationship with foaming time. That because the crystallinity is mostly dependent on chemical composition, all the samples prepared in this experiment are composed by 95% PVDF and 5% PVP. When foaming conditions change, the cell size and cell density alter greatly. However, the crystal form almost remains invariant, and the crystallinity of the composite affected litter within the margin of error.

Electrical Property of PVDF/PVP Composite Foams

The dielectric constant of the as-prepared PVDF/PVP composite foams is governed by the intrinsic dielectric constant of PVDF/PVP composite matrix and the morphology of the porous structure. Samples produced at different temperature were taken as example to explore the relationship between material electrical property and preparation condition. 95 wt % PVDF and 5 wt % PVP composites without

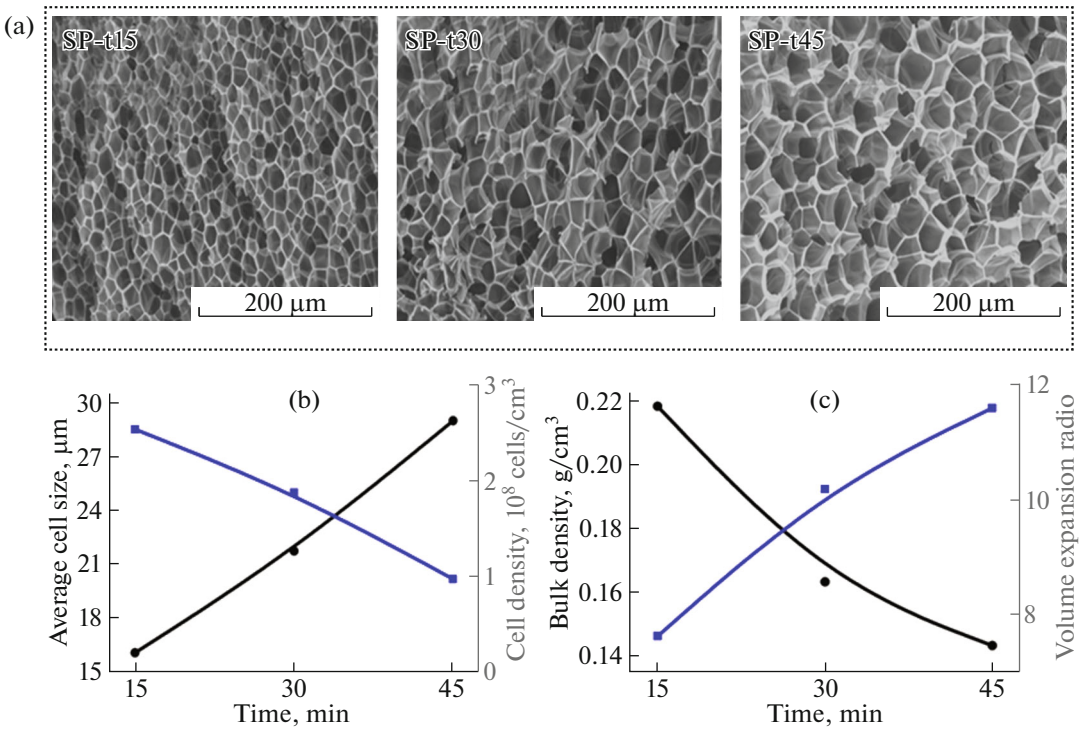

Fig. 5. (Color online) (a) SEM images of PVDF/PVP foams produced with different foaming time; (b) average cell size and cell density of PVDF/PVP foams produced with different foaming time; (c) the bulk density and volume expansion ratio of PVDF/PVP foams produced with different foaming time.

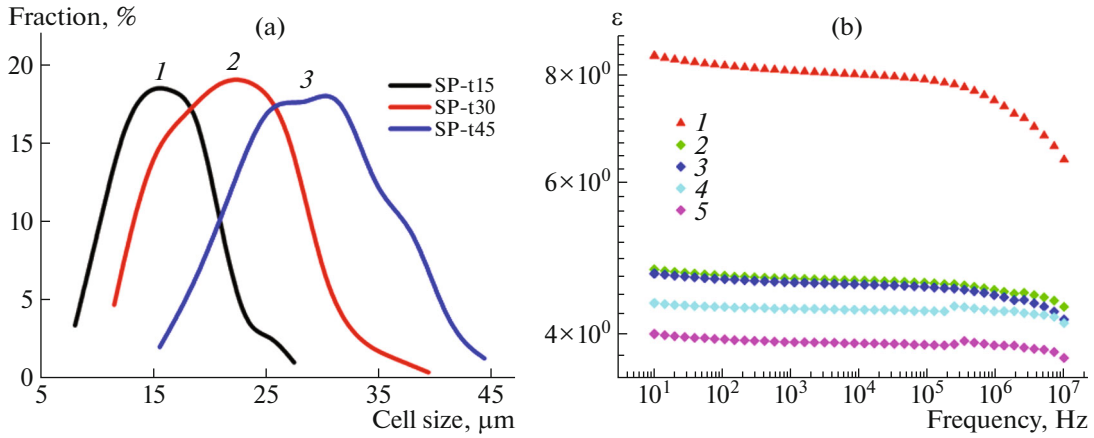

Fig. 6. (Color online) (a) The cell size distribution of PVDF/PVP foams produced with different foaming time: (*1*) SP-t15, (*2*) SP-t30, (*3*) SP-t45; (b) dielectric constant variation with respect to frequency for PVDF/PVP composite foams prepared at different temperature: (*1*) SP-T0, (*2*) SP-T200, (*3*) SP-T210, (*4*) SP-T220, (*5*) SP-T230.

foaming was named as SP-T0 as comparison. Figure 6b shows the dielectric constant with respect to frequency for PVDF/PVP composite foams. For SP-T0, the dielectric constant is about 8.4 at 10 Hz under ambient condition. As anticipated, all the porous PVDF/PVP composite foams exhibit considerably lower dielectric constants compared with PVDF/PVP composites without foaming (SP-T0). What's more, the dielectric constants of the porous foams steadily decreased with increasing foaming temperature. SP-T230 produced at foaming temperature of 230°C only obtained a dielectric constant of about 4.0, which was much lower than that of SP-T0. The drop in the dielectric constant is a natural result of the introduction of air that possesses a dielectric constant nearly unity. It is reasonable that, foams with higher volume expansion ratio achieve lower dielectric constant value. It also can be seen that, with increasing fre-

quently, PVDF/PVP composite foams are shown to be less sensitive. While for SP-T0 without foaming, the dielectric constant decreased to 6.3 at 10 MHz.

CONCLUSIONS

In conclusion, we systematically studied the effect of foaming conditions including saturation pressure, foaming temperature and foaming time on PVDF/PVP foams morphology, thermal and electrical behavior. The experimental results reveal that the competition between the cell growth and cell nucleation play an important role in average cell size and cell density. Uniform cells were observed at all conducted experimental conditions. At a very low saturation pressure, like 12 MPa, the cell density was low, and the average cell size was decreased because of the limited amount of $ScCO_2$ dissolved in PVDF/PVP composite. As increasing saturation pressure, the average cell size increased first, and then decreased due to the competition between cell growth and nucleation. With increasing foaming temperature, the system viscosity decreased and the composite became soft enough, thus increased cell size and decreased cell density, both in nearly linear manner observed. The variation of foaming time was considered to be closely related to the time for cells to grow. Thus, the results revealed that the average cell size enhanced when extending foaming time. The effect of processing condition on thermal behavior for PVDF/PVP foams was sight and the as-prepared microstructure foams showed out stable thermal property like bulk PVDF material. And the dielectric constant of PVDF/PVP composite foams decreased greatly compared with neat PVDF/PVP composite. What's more, with increasing volume expansion ratio, the dielectric constant of the prepared foams decreased.

ACKNOWLEDGMENTS

The authors appreciate financial supports from Education Department of Zhejiang Province (no. Y201738721), College Scientific Research Project of Jiaxing Nanyang Polytechnic Institute (no. pg30017ky001).

REFERENCES

1. C. H. Lee, N. Johnson, J. Drelich, and Y. K. Yap, Carbon **49**, 669 (2011).
2. P. S. Brown, O. D. L. A. Atkinson, and J. P. S. Badyal, ACS Appl. Mater. Interfaces **6**, 7504 (2014).
3. H. Y. Araghi and M. F. Paige, Langmuir **27**, 10657 (2011).
4. L. Chen, M. Liu, L. Lin, T. Zhang, J. Ma, Y. Song, and L. Jiang, Soft Matter **6**, 2708 (2010).
5. Y. Cao, N. Liu, C. Fu, K. Li, L. Tao, L. Feng, and Y. Wei, ACS Appl. Mater. Interfaces **6**, 2026 (2014).
6. A. M. Stephan, N. G. Renganathan, S. Gopukumar, and T. Dale, Mater. Chem. Phys. **85**, 6 (2004).
7. E. Reverchon, E. S. Rappo, and S. Cardea, Polym. Eng. Sci. **46**, 188 (2006).
8. E. Reverchon and S. Cardea, J. Supercrit. Fluids **35**, 140 (2005).
9. A. R. C. Duarte, J. F. Mano, and R. L. Reis, J. Bioact. Compat. Polym. **24**, 385 (2009).
10. G. Han, S. Zhang, X. Li, N. Widjojo, and T. S. Chung, Chem. Eng. Sci. **80**, 219 (2012).
11. Y. Tao, Q. Xue, Z. Liu, M. Shan, C. Ling, T. Wu, and X. Li, ACS Appl. Mater. Interfaces **6**, 8048 (2014).
12. G. Wei, H. Yu, X. Quan, S. Chen, H. Zhao, and X. Fan, Environ. Sci. Technol. **48**, 8062 (2014).
13. D. G. Kim, H. Kang, S. Han, and J. C. Lee, ACS Appl. Mater. Interfaces **4**, 5898 (2012).
14. H. J. Kim, K. Choi, Y. Baek, D. Kim, J. Shim, J. Yoon, and J. Lee, ACS Appl. Mater. Interfaces **6**, 2819 (2014).
15. L. Huang, J. T. Arena, S. S. Manickam, X. Jiang, B. G. Willis, and J. R. McCutcheon, J. Membr. Sci. **460**, 241 (2014).
16. W. Choi, J. Choi, J. Bang, and J. H. Lee, ACS Appl. Mater. Interfaces **5**, 12510 (2013).
17. A. Huang, Q. Liu, N. Wang, and J. Caro, J. Mater. Chem. A **2**, 8246 (2014).
18. X.-L. Li, L.-P. Zhu, J.-H. Jiang, Z. Yi, B.-K. Zhu, and Y.-Y. Xu, Chin. J. Polym. Sci. **30**, 152 (2011).
19. J. H. Jiang, L. P. Zhu, H. T. Zhang, B. K. Zhu, and Y. Y. Xu, J. Membr. Sci. **457**, 73 (2014).
20. C. Li, Z. Du, W. Zou, H. Li, and C. Zhang, React. Funct. Polym. **88**, 24 (2015).
21. L. Chen, G. Liu, S. Liu, L. Bai, and Y. Wang, J. Biomater. Sci., Polym. Ed. **25**, 1306 (2014).
22. G. Ji, W. Zhai, D. Lin, Q. Ren, W. Zheng, and D. Jung, Ind. Eng. Chem. Res. **52**, 6390 (2013).
23. D. Rende, L. S. Schadler, and R. Ozisik, J. Chem. **2013**, 1 (2013).
24. G. Yang, J. Gao, X. Hu, C. Geng, and Q. Fu, J. Supercrit. Fluids **73**, 1 (2013).
25. F. Liu, N. A. Hashim, Y. Liu, M. R. M. Abed, and K. Li, J. Membr. Sci. **375**, 1 (2011).
26. C. H. Shih, C. C. Gryte, and L. P. Cheng, J. Appl. Polym. Sci. **96**, 944 (2005).
27. S. Cardea and E. Reverchon, Chem. Eng. Process. **50**, 630 (2011).
28. Z. Cui, N. T. Hassankiadeh, S. Y. Lee, J. M. Lee, K. T. Woo, A. Sanguineti, V. Arcella, Y. M. Lee, and E. Drioli, J. Membr. Sci. **444**, 223 (2013).
29. M. G. Buonomenna, P. Macchi, M. Davoli, and E. Drioli, Eur. Polym. J. **43**, 1557 (2007).
30. T. Cai, W. J. Yang, K. G. Neoh, and E. T. Kang, Ind. Eng. Chem. Res. **51**, 15962 (2012).
31. A. Bottino, G. Capannelli, O. Monticelli, and P. Piaggio, J. Membr. Sci. **166**, 23 (2000).
32. D. J. Lin, C. L. Chang, C. K. Lee, and L. P. Cheng, Eur. Polym. J. **42**, 2407 (2006).